Preprint Title	Effects of substrate stiffness on the viscoelasticity and migration of prostate cancer cells by atomic force microscopy
Authors	Xiaoqiong Tang, Yan Zhang, Jiangbing Mao, Yuhua Wang, Zhenghong Zhang, Zhengchao Wang and Hongqin Yang
Publication Date	14 März 2022
Article Type	Full Research Paper
Supporting Information File 1	Supporting Information.docx; 2.3 MB
ORCID® iDs	Jiangbing Mao - https://orcid.org/0000-0003-0932-0847; Hongqin Yang - https://orcid.org/0000-0002-7794-5921

Effects of substrate stiffness on the viscoelasticity and migration of prostate cancer cells by atomic force microscopy

Xiaoqiong Tang‡[1], Yan Zhang‡[1], Jiangbing Mao[1], Yuhua Wang[1], Zhenghong Zhang[2], Zhengchao Wang*[2] and Hongqin Yang*[1]

[1] Key Laboratory of Optoelectronic Science and Technology for Medicine of Ministry of Education, Fujian Provincial Key Laboratory for Photonics Technology, Fujian Normal University, Fuzhou 350007, China

[2] Fujian Provincial Key Laboratory for Developmental Biology and Neurosciences, College of Life Sciences, Fujian Normal University, Fuzhou 350007, China

Email:

Zhengchao Wang* - zcwang@fjnu.edu.cn (Z.W.)

Hongqin Yang* - hqyang@fjnu.edu.cn (H.Y.)

* Corresponding author

‡ Equal contributors

Abstract

The stiffness of the extracellular matrix of tumour cells plays a key role in tumour cell metastasis. However, it is unclear how mechanical properties regulate the cellular response to the matrix environmental. In this study, atomic force microscopy and laser confocal imaging were used to qualitatively quantify the relationship between substrate stiffness and the migration of prostate cancer (PCa) cells. Cells cultured on stiff substrate (35kPa) undergone severval interesting phenomena compared to soft substrate (3kPa). Here, the stimulation of the stiff substrate promoted the F-actin skeleton filaments into bundles and increased the polarity index of the external contour of PCa cells. Analysis of AFM force distance curves indicated that the elasticity of cell cultured on 35kpa increased while the viscosity decreased. Wound-healing experiments showed that PCa cells cultured on 35kpa have higher potential of migration. These phenomena suggested that the mechanical properties may correlate to the migration of PCa cells. After depolymerization of actin, the elasticity of PCa cell decreased while the viscosity increased, and the migration ability was correspondingly weakened. In conclusion, this study clearly demonstrated the relationship between substrate stiffness and the mechanical properties of cells in prostate tumor metastasis which provides a basis for understanding the changes in the biomechanical properties at the single-cell level.

Keywords

Atomic force microscopy; substrate stiffness; prostate cancer cells; cytoskeleton; viscoelasticity; migration

Introduction

Prostate cancer is a common malignancy of the male urinary tract and has become the second most threatening cancer to men's health after lung cancer[1, 2].Clinical data indicate that 90% of patients have a survival rate of more than 10 years if the prostate tumour is located in the prostate at the time of diagnosis and there are no distant metastases[3, 4].However, most patients with high-risk PCa have a poor prognosis or even clinical treatment failure due to the occurrence of distant metastases[5, 6].Therefore, the study of the mechanisms of metastasis is of great importance to the clinical management of PCa.

There are many factors that mediate tumour metastasis. Of these, the extracellular matrix (ECM) is most closely associated with tumour metastasis. ECM is made up of extracellularly secreted macromolecules. It not only contains a large number of biochemical factors, but also provides a suitable mechanical environment for cells, including physical signals such as substrate stiffness, hydrostatic pressure, shear stress, strain, pressure and tension[7-9].These mechanical factors play an important role in regulating normal cellular physiological functions and the development of disease. Studies have shown that solid tumourigenesis and metastasis are often accompanied by abnormal ECM cross-linking, remodelling and increased tissue stiffness[10].Peng et al. observed that substrate stiffness directly activates integrin β1 and adherent spot kinase, accelerates the maturation of focal adhesions and induces a downstream cascade of intracellular signals in the RhoA/ROCK pathway, thereby promoting breast cancer cell motility[11].Dai et al. found that high stiffness matrix regulates the morphology of MG63 osteosarcoma cells, promotes actin polymerization and nuclear accumulation of cardiomyosin-related transcription factor A, induces epithelial-mesenchymal transition (EMT) in osteosarcoma cells and thus

promotes osteosarcoma metastasis[12].Differences in ECM stiffness do not only affect the development of breast cancer and osteosarcoma. Recent studies on pancreatic and hepatocellular carcinoma have also found that harder ECM promotes EMT[13, 14].Therefore, the study of ECM stiffness has important implications for tumour metastasis.

For prostate cancer, the current clinical approach to improving positive puncture rates is to incorporate ultrasound elastography, which imaging based on the difference in stiffness between the lesion and the adjacent tissue. It was found that a high stiffness external environment promotes PC3 cell migration and proliferation by inducing yes-associated protein and tafazzin (YAP/TAZ) nuclear localisation, suggesting that the behaviour of PCa cells is regulated by the external environment[15].Traditional biological approaches to studying prostate cancer are based on molecular genetics and gene signalling. However, the cellular mechanistic properties that allow cells to express various biological functions have not been well appreciated[16].In recent years, alterations in the physical properties of cells have been considered as a marker of malignant transformation of cancer cells[17-19].Based on atomic force microscopy, our group found that the disease progression of prostate cancer tissue is related to its biomechanical properties, that the higher the pathological grade of prostate cancer tissue, the less elastic and viscous it is, indicating that the mechanical properties of the tissue can predict the pathological grade of prostate cancer. This is consistent with the pathological diagnosis of transrectal ultrasound biopsy, suggesting that changes in the mechanical properties of prostate cancer are closely related to tumour metastasis[20].However, the relationship between the regulation of cell behaviour by the extracellular environment and the mechanical properties of the cells themselves has never been discussed in detail.

In this study, polyacrylamide hydrogel substrates with different stiffness values (3-35 kPa) were prepared to simulate the stiffness of normal and prostate cancer tissues[21-23].Combined with confocal microscopic imaging techniques and atomic force microscopic imaging, the changes in the mechanical properties of the cells themselves during cell migration were investigated by regulating the substrate stiffness. The results contribute to the understanding of the relationship between substrate stiffness and prostate cancer metastasis and possible regulatory mechanisms, which can further guide the study and treatment of cancer metastasis.

Results and Discussion

Effect of substrate stiffness on the migration of prostate cancer cells

In order to investigate the mechanical properties and metastatic ability of human prostate cancer cells in different external environments of the cells themselves. Polyacrylamide hydrogel substrates with adjustable stiffness were prepared by controlling the concentration of acrylamide and bisacrylamide (Figure 1). The stiffnesses were 3 kPa (soft group) and 35 kPa (stiff group), representing normal prostate tissue and tumour tissue, respectively, and 19 kpa, an intermediate transition group. We first tested the toxicity of the hydrogel substrates to the cells and found that all three stiffness substrates were non-toxic to the cells and the cells were most active after 48 hours of incubation (Figure S1). After culturing the cells on the substrates for 48 hours, we measured the ability of the cells to migrate in the hydrogels for 24 hours to ensure that the cells were in a stable state in the hydrogels (Figure 2a). We observed that the rate of cell migration in the hydrogel was stiffness dependent. As the stiffness of the substrate increased, the cell migration rate also

increased. Specifically, compared to HPV-PZ-7 cells, on a stiff substrate (35 kPa), PC3 cells moved in a sheet-like fashion and nearly closed the gap. Cells at 19 kPa stiffness had the next lowest migration capacity, and cells on soft substrates (3 kpa) had the weakest migration capacity (Figure 1c). Cell proliferation assays also revealed that both strains of cells had a significantly greater ability to proliferate on stiff substrates, and that the proliferation of prostate cancer cells increased significantly with increasing substrate stiffness. (Figure S2a-b). Considering that the migration assay and proliferation assay were performed by culturing the cells on the substrate for 48 h, digesting them and then inoculating them in 6 and 96 well plates. It suggests that the effect of substrate on cells for 48h has altered the internal mechanical properties of the cells and is no longer solely caused by the external physical environment. Invasion experiments revealed that cells on stiff substrates were more aggressive, with more cells crossing the upper chamber, compared to cells on other substrates (Figure 2b and d). Soft substrates appear to give the cells a suitable attachment site, allowing little movement. Their behaviour exhibited a lesser role with the cellular substrate. Our study suggests that sclerosis of the extracellular matrix enhances the growth and viability of cancer cells and can promote their migration and invasion.

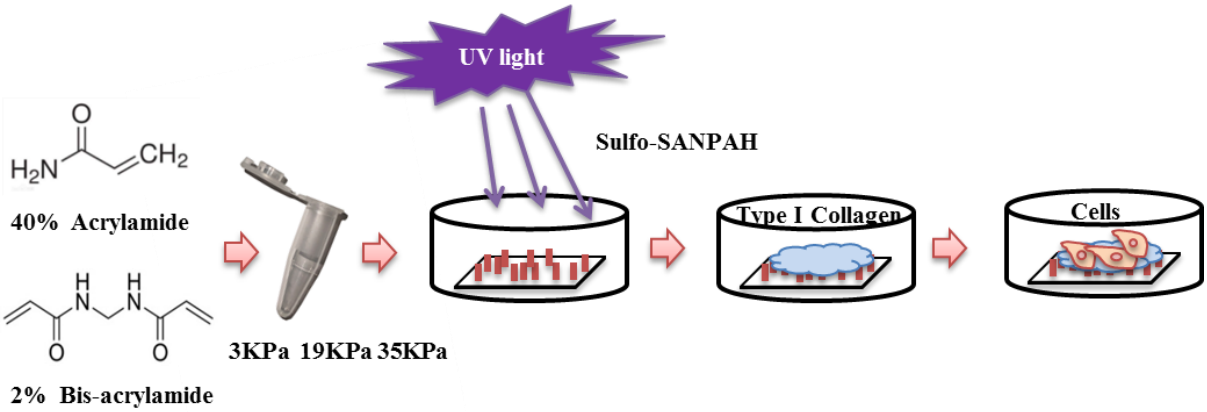

Figure 1: Schematic diagram of polyacrylamide hydrogel substrate preparation and cell culture process.

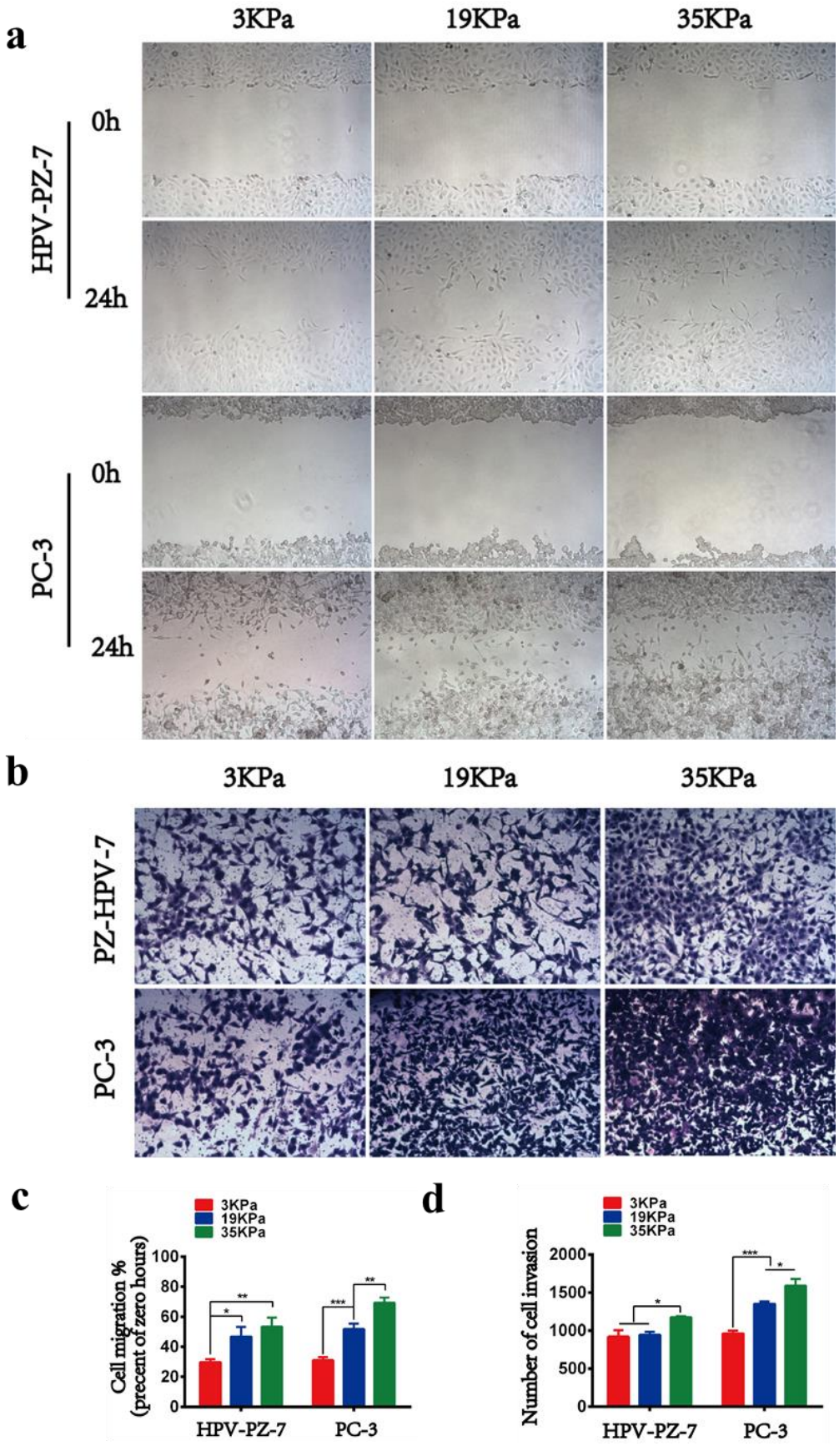

Figure 2: Effect of substrate stiffness on the migration of prostate cancer cells. (a) Analysis of cell wound healing of HPV-PZ-7 and PC 3 cells on different stiffness substrates. (b) Transwell analysis of the invasion ability of HPV-PZ-7 and PC 3 cells on different stiffness substrates. (c) Quantitative statistics on the migration ability of HPV-PZ-7 and PC 3 cells on different substrates. (d) Quantitative statistics of the invasion ability of HPV-PZ-7 and PC 3 cells on different substrates. * P <0.05, *** p <0.001.

Morphological analysis showed different characteristics in different stiffnesses

Differences in cell motility in different stiffness hydrogels are inevitably limited by the physical limitations of the hydrogel, which most visually affects the morphology of the cells. When HPV-PZ-7 and PC3 cells were cultured in hydrogels of different stiffnesses for 48 hours, we observed by analysis of phase contrast microscopic images that most cells on stiff substrate were elongated and had a higher degree of cell expansion. In contrast, the cells on the soft substrates were rounded and had a lower degree of cell expansion (Figure 3a). By measuring the cell surface area, perimeter and polarity index, it was found that an increase in substrates stiffness was positively correlated with cell expansion. There was a significant difference between the surface area and perimeter of HPV-PZ-7 and PC3 cells on stiff and soft substrates (Figure S2a-b). The polarity index showed that PC3 cells were more polar on stiff substrates, while HPV-PZ-7 cells were not sensitive to substrate stiffness (Figure 3b). The stiffer the hydrogel substrate, the greater the polarity index of the cancer cells. This suggests that the cell polarity index can be an indicator of how cells respond to the extracellular environment. This finding is consistent with previously reported results [24, 25]. The significant polygonal shape of cells is widely believed to be associated with enhanced migration and invasion. Of these, round cells spread more slowly, whereas long cells, morphologically due to their resemblance to fibroblasts, have prominent leading edges and retractable tails, and therefore exhibit greater flexibility[26].The micro-nano morphological imaging of the cell membrane in different stiffness extracellular environments is shown in Figure 3c. The leading edge of the PC3 cell membrane on stiff substrates is prominent, with a more pronounced ridge-like protrusion on the surface of the cell pseudopod. In contrast, the surface of PC3 cells on soft substrates was smoother. In addition, both cell strains on the stiff substrate were observed to be taller than those on the other two substrates, ranging from 1-4 μm. The height of the HPV-PZ-7 cells was highest on the stiff substrate,

indicating that normal cells were largely invasive at this stiffness. In contrast, the height difference between PC3 cells on stiff substrates and the other two stiffnesses was only about 1 μm, indicating that prostate cancer cells are more sensitive to extracellular substrate stiffness. All these phenomena suggest that a stiff extracellular environment contributes to the protrusion and extension of the leading edge of the cancer cells. As the formation of filamentous pseudopods is thought to be crucial for cell invasion [25, 26]. Our results suggest that stiff substrates promote the protrusion of the leading edge of cancer cell membranes to guide cell motility. The average surface roughness of cells in different stiffness extracellular environments is shown in Figure 3d. PC3 cells showed a higher average surface roughness (Ra) on stiff substrates than on soft substrates, in contrast to HPV-PZ-7 cells, which did not exhibit this feature. Peak-to-valley ratio roughness (Rt) and root mean square surface roughness (Rq) also showed the same characteristics, see Supplementary Figure 2c-d. Cell surface roughness is a quantitative measure of the variability of cell surface topography and serves as an indicator to assess the state of the cell that the greater the roughness, the greater the undulation of the cell surface topography[27]. It can be involved in many cellular behaviours such as cell migration and adhesion and is an important indicator of the physiological state of cells [28, 29]. Thus, stiff substrates do promote migration of prostate cancer cells by altering their morphology, including cellular polarity index, filamentous pseudopods and surface roughness.

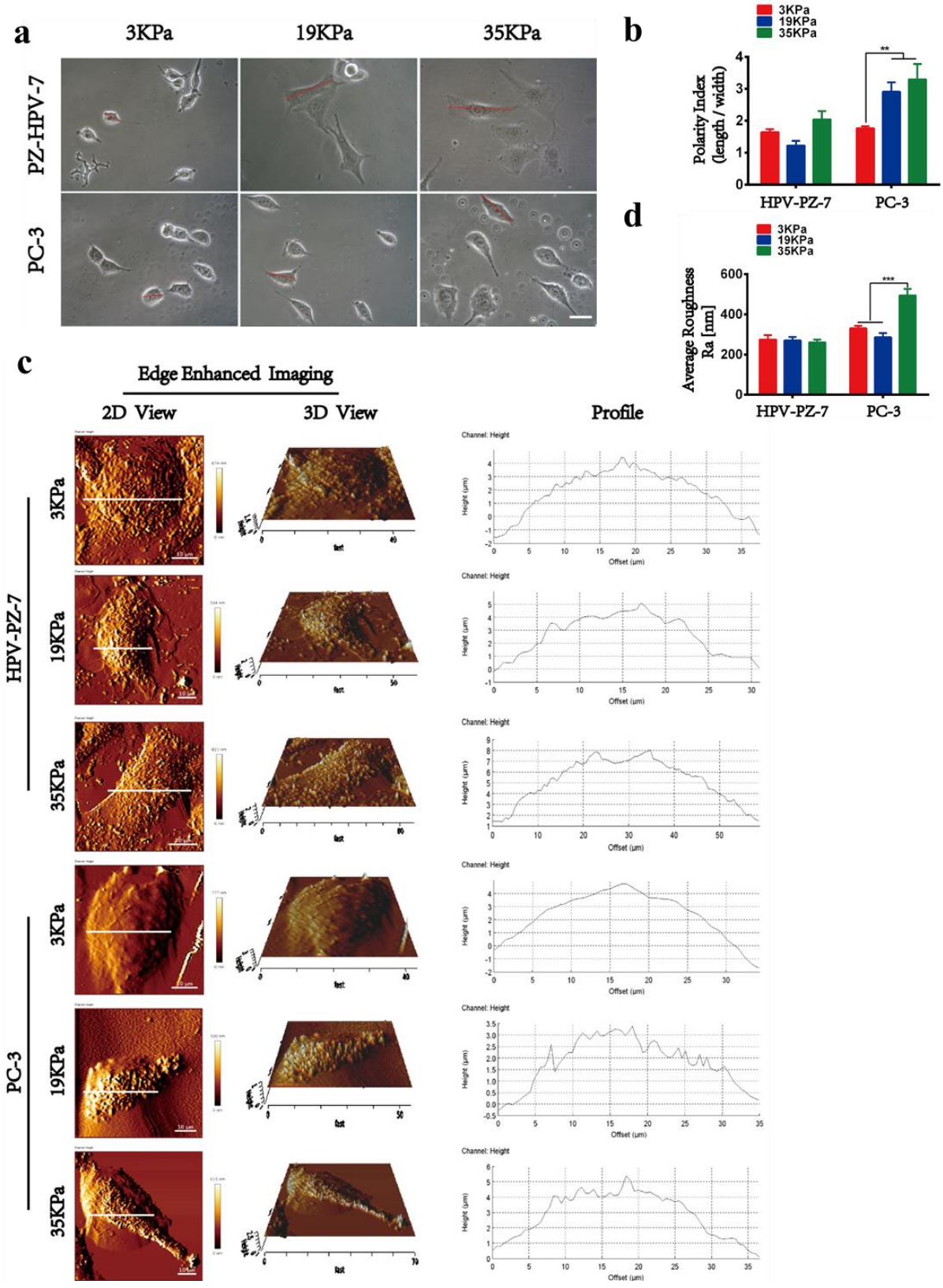

Figure 3: Morphological analysis showed different characteristics in different stiffness. (a) Phase contrast microscope imaging of PZ-HPV-7 and PC 3 cells on different stiffness substrates, scale bar = 10μm; (b) Quantitative statistical graph of

cell polarity index (length/width); (c) Atomic force microscopy imaging of HPV-PZ-7 and PC 3 cells on different stiffness substrates. From left to right, the edge-enhanced images of cells are displayed, including two-dimensional and three-dimensional imaging and cell contour maps; (d) The quantitative statistics of the average surface roughness (Ra). ** $p < 0.01$, *** $p < 0.001$.

Skeletal microfilaments respond to changes in substrate stiffness on prostate cancer cells

We further consider how the role of cell sensing substrates makes cancer cells more capable of migrating on stiff substrates. The distribution and content of F-actin in the cells was examined using fluorescent isothiocyanate (FITC)-labelled phalloidin to analyse the distribution and local directional changes of filamentous actin. It could be seen that the microfilaments of PC3 cells were densely arranged and ordered on the stiff substrate, with the strongest fluorescence intensity, which was significantly higher than that of HPV-PZ-7 cells. In addition, PC3 cells were found to have distinct filamentous pseudopods on the stiff substrates (Figure 4a-c), which was consistent with the results obtained from micro-nanomorphic imaging of the cell membrane. We obtained that prostate cancer cells exhibit a strong migration ability by sensing changes in the extracellular environment through actin polymerization and filamentous pseudopods. This is because the role of actin polymerisation in cell adhesion structure formation, maturation and myosin contraction has been found to be an important factor in cell migration[30-32].Cytoskeletal myosins drive cell contraction and enhance the longitudinal tension of the cell causing the cell to contract in the direction of cell migration, resulting in the displacement of the entire cell[33-35].

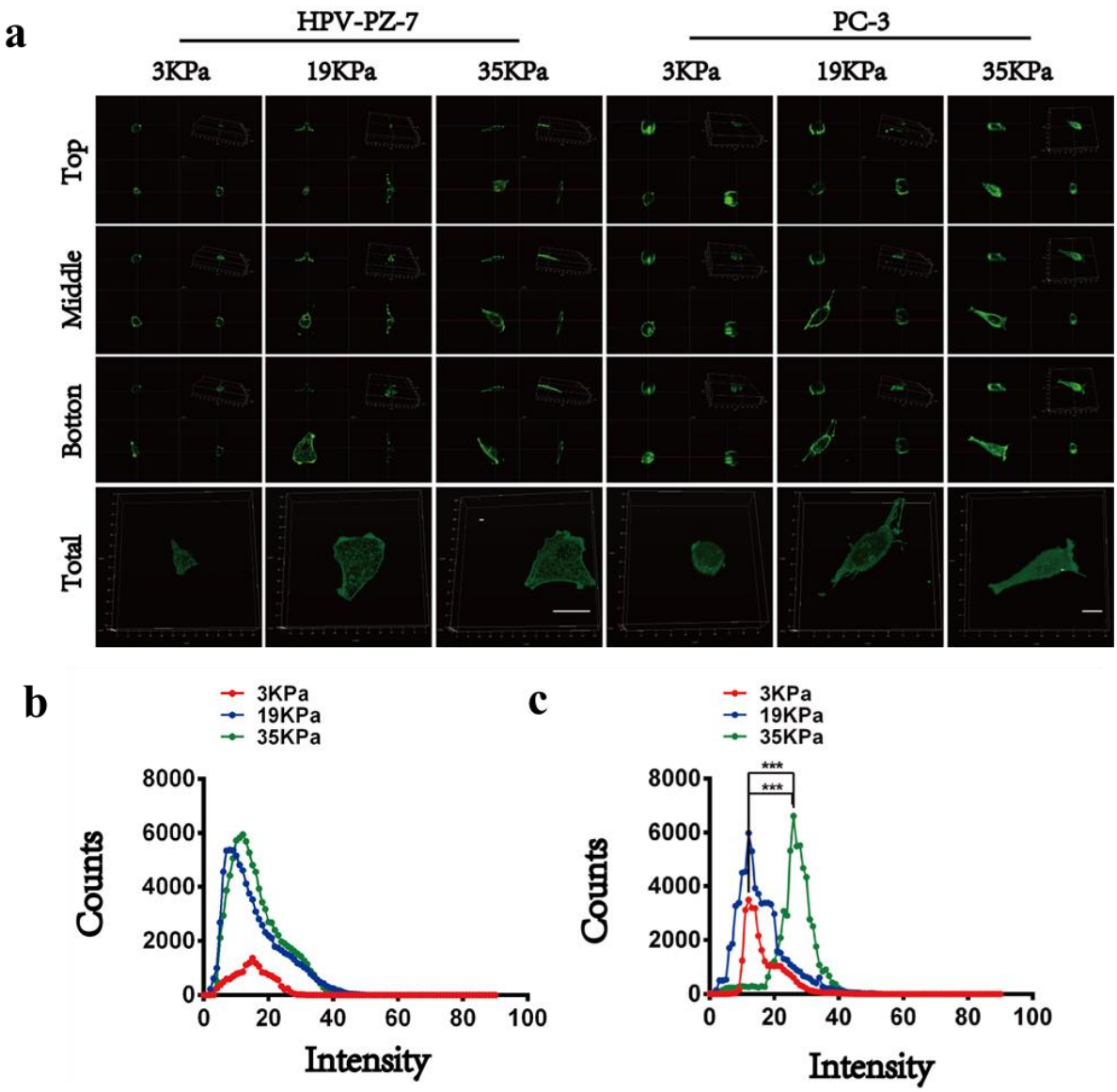

Figure 4: Skeletal microfilaments respond to changes in substrate stiffness on prostate cancer cells. (a) Three-dimensional fluorescence images of HPV-PZ-7 and PC 3 cytoskeletal microfilaments on different stiffness substrates; the scale of HPV-PZ-7 cells is 20 μm, and the scale of PC 3 cells is 10 μm; (b) Fluorescence intensity distribution of HPV-PZ-7 cells on different stiffness substrates; (c) Fluorescence intensity distribution of PC 3 cells on different stiffness substrates. *** p <0.001.

Mechanical properties respond to the effect of substrate stiffness on prostate cancer cells

The previous experiments have shown that stiff substrates promote prostate cancer cell migration by altering cell morphology and actin distribution, so what are the mechanical properties of the cells themselves in response to the action of the substrate? Nanoscale AFM was used to measure changes in the elasticity of live cells in situ and to quantify the mechanical response of the extracellular environment to HPV-PZ-7 and PC3 cells with different stiffnesses. To overcome the effect of different indentation depths on elasticity, we measured the cells in the same area and at the same force. PC3 cells were found to have significantly lower elasticity values than HPV-PZ-7 cells, indicating that prostate cancer cells are less stiff than normal cells. This is consistent with previous reports on other cells[36, 37].Moreover, we found that the higher the substrate stiffness, the higher the cellular elasticity values, suggesting that the spreading of the cells has an effect on their mechanical properties, with cells that are adequately spread being stiffer than those that are less spread (Figure 5a and d). Furthermore, considering the rheological behaviour of the living cells themselves, which the energy dissipated during the downward pressure of the probe to deform and recover the cells from deformation[38, 39],this energy dissipation was mainly caused by cell adhesion that was a certain separation between the approach and retraction curves (Figure 5c).The results showed a negative correlation between viscosity values and substrate stiffness in PC3 cells that the higher the substrate stiffness, the lower the cell viscosity, whereas HPV-PZ-7 cells did not show this characteristic (Figure 5b and e). The physical quantity expressed by viscosity is inversely proportional to mobility. The lower the viscosity, the more mobile it is, and the mobility of the cells is positively correlated with their ability to invade. Thus, prostate cancer cells respond to the effects of their extracellular environment by altering their mechanical properties (both elasticity and viscosity) and thus their ability to migrate. Changes in the mechanical properties of

the cells themselves are closely related to differences in their extracellular environment, which are determined by the tension and structural organisation of the cytoskeleton[33, 34]. Our results seem to indicate that the cytoskeleton plays an important role in mediating migration capacity in different extracellular environments.

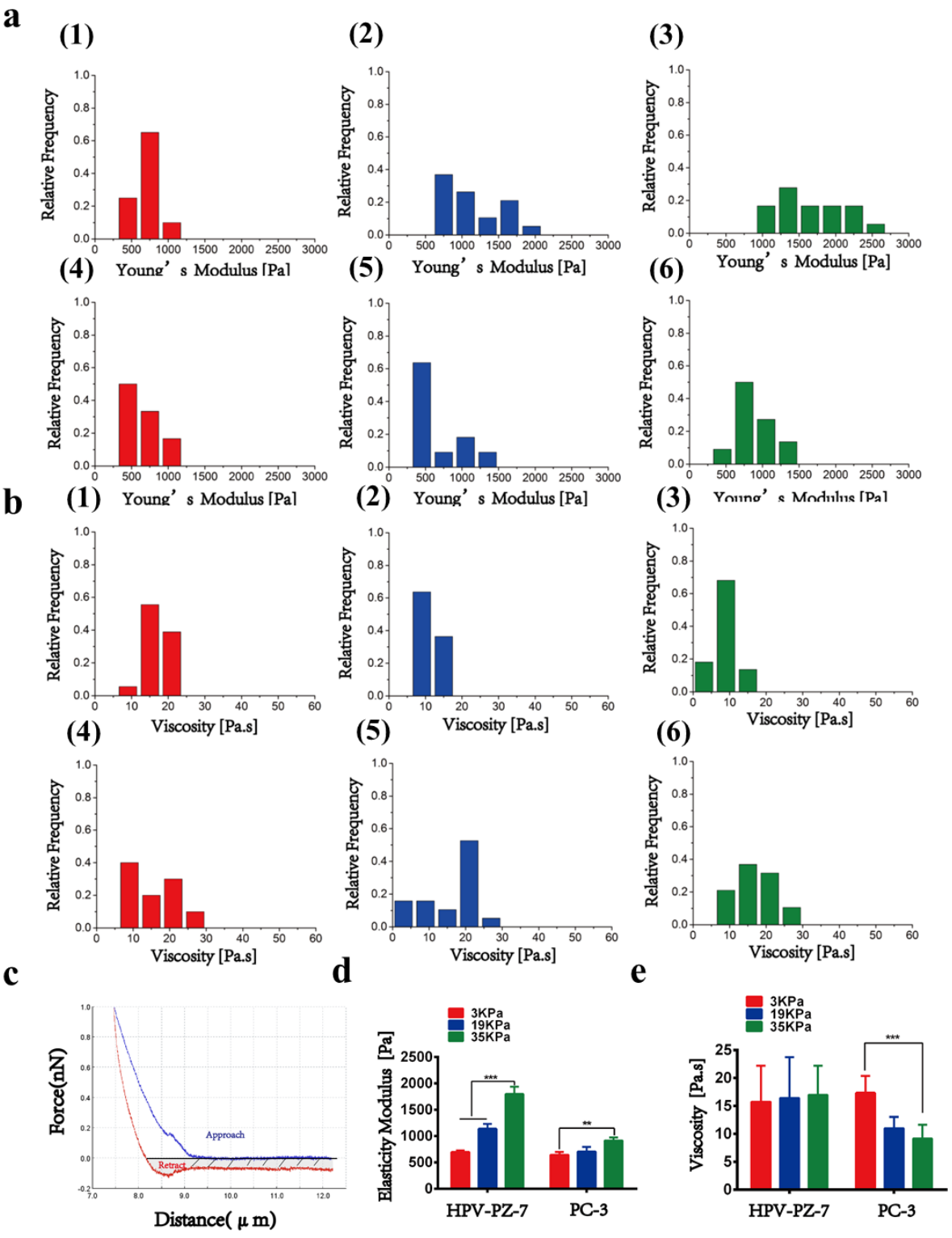

Figure 5: Mechanical properties respond to the effect of substrate stiffness on prostate cancer cells. (a) Histogram of the elastic frequency distribution of HPV-PZ-7 and PC 3 cells on different stiffness substrates. Among them (1), (2), (3) are the histograms of the elastic frequency distribution of HPV-PZ-7 cells at 3, 19, and 35kPa, respectively. (4), (5), (6) are the histograms of the elastic frequency distribution of PC 3 cells at 3, 19, and 35kPa, respectively. (b) Histogram of the viscosity frequency distribution of HPV-PZ-7 and PC-3 cells on different stiffness substrates. Among them, (1), (2), and (3) are the histograms of the viscosity frequency distribution of HPV-PZ-7 cells at 3, 19, and 35 kPa, respectively. (4), (5), (6) are the histograms of the viscosity frequency distribution of PC 3 cells at 3, 19, and 35 kPa, respectively;(c) Force-distance graph of cells. (d) The average elasticity value of HPV-PZ-7 and PC 3 cells on substrates of different stiffness.(e) The average viscosity value of HPV-PZ-7 and PC 3 cells on substrates of different stiffness. ** $p < 0.01$, *** $p < 0.001$.

Substrate stiffness affects PCa cell migration via skeleton microfilament and mechanical properties

To further determine whether substrate stiffness affects prostate cancer cell migration by influencing cytoskeletal microfilaments. We treated the cells with Blebbistatin, a non-muscle myosin type II ATPase inhibitor. 20uM Blebbistatin treatment for 30min revealed disorganised microfilament bundles on stiff substrates and weaker fluorescence intensity in PC3 cells than in non-Blebbistatin treated cells (Figure S4a-c). The Young's modulus of HPV-PZ-7 and PC3 cells on stiff substrates was reduced after Blebbistatin treatment, with no effect on soft substrates. However, prostate cancer cells on stiff substrates continued to exhibit high elasticity (Figure 6a and c). The viscosity data showed an increase in viscosity values for PC3 cells on stiff substrates after Blebbistatin treatment (Figure 6b and d). The results indicate an overall decrease in cell stiffness after Blebbistatin action, but the 35 KPa stiffness substrates continued to show a mechanical response given the possible Blebbistatin duration of action factor. The results of migration and invasion assays showed that the migration and invasion abilities of both cells on different stiffness substrates were reduced compared to those without Blebbistatin treatment (Figure S5a-d). The results show that when we depolymerise actin polymerisation with an actin-binding protein inhibitor, the actin fibrils fail to polymerise into bundles and the prostate cancer cells themselves have reduced elasticity values and increased viscosity values, thus reducing the migration ability of the prostate cancer cells.

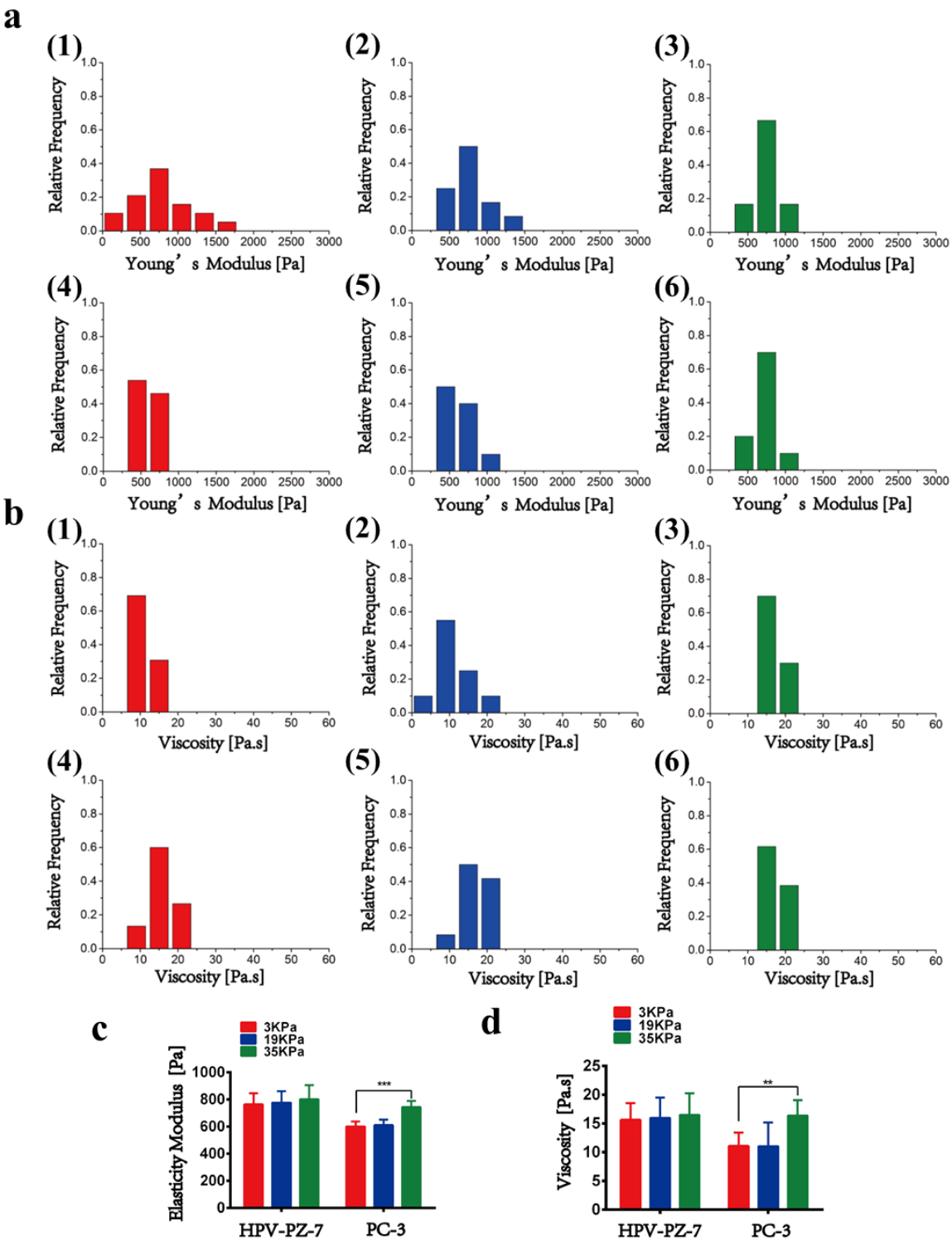

Figure 6: The effect of Blebbistatin on the viscoelasticity of PCa cells. (a) Histogram of elastic frequency distribution of HPV-PZ-7 and PC 3 cells on substrates with different stiffness after Blebbistatin treatment. Among them, (1), (2), (3) are the histograms of the elastic frequency distribution of HPV-PZ-7 cells at 3, 19, and 35

kPa, respectively. (4), (5), (6) are the histograms of the elastic frequency distribution of PC 3 cells at 3, 19, and 35 kPa, respectively.(b) Histogram of the viscosity frequency distribution of HPV-PZ-7 and PC 3 cells on substrates with different stiffness after Blebbistatin treatment. Among them, (1), (2), and (3) are the histograms of the viscosity frequency distribution of HPV-PZ-7 cells at 3, 19, and 35 kPa, respectively. (4), (5), (6) are the histograms of the viscosity frequency distribution of PC 3 cells at 3, 19, and 35 kPa, respectively; (c) The average elasticity value of HPV-PZ-7 and PC 3 cells on substrates of different stiffness after Blebbistatin treatment.(d) The average viscosity value of HPV-PZ-7 and PC 3 cells on substrates of different stiffness after Blebbistatin treatment. ** $p < 0.01$, *** $p < 0.001$.

Conclusion

To our knowledge, the present study qualitatively quantified for the first time the association of viscoelastic properties measured by using atomic force microscopy with the migration under substrate stiffness of PCa cells. On stiff substrate, the F-actin skeleton filaments into bundles and increased the elasticity while the viscosity decreased of PC3 cells to enhance their migration ability. Furthermore, the results of treatment with the actin inhibitor suggested that the response of PCa cells to the matrix environmental may be caused by differences in F-actin cytoskeleton that lead to changes in the mechanical properties of the cell. Since nanomechanical properties can be used as an indicator of cancer cell migration, this study may provide a new approach to investigate the migration mechanism of PCa cells. As well as cytoskeleton-mediated migration of PCa cells may be useful for cancer therapeutic drug screening and development.

Experimental

Cell culture

PZ-HPV-7 normal human prostate epithelial cells and PC 3 cancerous prostate cells were purchased from Shanghai ATCC cell bank. PZ-HPV-7 and PC 3 were cultured respectively in Dulbecco's Modified Eagle Medium medium containing 10% fetal bovine serum (FBS) and 1% penicillin-streptomycin solution and Ham's F-12K containing 10% FBS and 1% penicillin-streptomycin solution. The cells were digested with 0.25% trypsin and counted, and then inoculated in cell culture dishes with different substrate stiffness.

Preparation of polyacrylamide (PAA) gel substrates

The preparation of polyacrylamide hydrogels with different stiffness refered to the experimental method of Justin R. TSE[40].In a nutshell, it's as follows. The cover glass with 25 mm diameter was uniformly covered with a thin layer of 0.1M NaOH and dried. After 5 min activation with 3-aminopropyl triethoxysilane (ServiceBio, China), sterile water was washed. The treated glass slides were immersed in 0.5% glutaraldehyde solution, placed at room temperature for 30 min, and then taken out to air dry. The slides were treated with dimethyldichlorosilane for 5 min, washed and dried.40% acrylamide and 2% bis-acrylamide (Sigma-Aldrich) were mixed in a certain proportion, followed by 10% ammonium persulfate and 0.1% TEMED. After the mixture was fully mixed, 25μl was absorbed onto the treated glass slide, and the treated cover glass was quickly covered. After the gel was cross-linked for about 20 min, the cover glass was lightly removed, placed in sterile water and stored at 4℃. The stiffness of the hydrogels with different proportions were shown in Table 1. Next, the gel was coated with Sulfo-SANPAH solution and activated in UV light at 365 nm for 10 min. These gels were then coated with type I collagen (0.1 $mg.ml^{-1}$) and

incubated overnight at 4°C. On the second day, the excess collagen solution was removed with sterile water, and then HPV-PZ-7 and PC 3 cells were inoculated on PPA substrates with different stiffness for 12h, 24h, 48h and 72h, respectively. The schematic diagram was shown in Figure 1A.

Table 1: Composition ratio of polyacrylamide hydrogel substrate with different stiffness

Sample	40% Acrylamide (ml)	2% Bis-acrylamide (ml)	H_2O	Elastic Modulus (kPa)
Soft	1.25	0.50	8.25	3.15 ± 0.85
Medium	2.00	1.32	6.68	19.66 ± 1.19
Stiff	2.50	1.50	6.00	34.88 ± 2.65

Cell death assay

Cells were stained with calcein-AM and propidium iodide (PI) to double stain the living and dead cells for analysis at the living and dead cell levels.HPV-PZ-7 and PC 3 cells (1×10^6 cells/ mL) were cultured on PAA hydrogels with different stiffness for 12h, 24h, 48h and 72h, respectively. Cell precipitation was collected by digestion and centrifugation. Assay Buffer was used to cleanse cells three times to remove residual esterase activity. Cells were incubated at 37℃ for 15 min in a Assay Buffer solution containing calcitrin-AM (1 μM) and PI (3 μM) and then imaged with a laser confocal microscope.

Cell migration and invasion assay

To assess cell migration, cells cultured on PAA gel with different stiffness for 48 h were removed by trypsinization and were seeded at a density of 2×10^6 cells/mL in six-well plates to a confluent monolayer. A 10ul pipet tip was used to scrape the cell

monolayer in a straight line to create an empty gap. The debris was then removed by washing the cells 3 times with PBS and then replaced with 2 mL of fresh medium without serum. Then, the cells were imaged immediately and 24 h after scratch. Results processing: Three locations in the image scratch were randomly selected, the width of cell scratch was measured and the average value was calculated. Cell migration index (Im=(G0-G1)/G0·100%) was used to represent the speed of cell migration. G0 referred to the scratch width at 0h in the image immediately after scratch.G1 referred to the scratch width of the image collected 24 hours after the scratch cell culture.

For the invasion assays, cells cultured on PAA gel with different stiffness for 48 h were removed by trypsinization and then seeded into the upper compartment (2×10^4 cells/well) of a transwell chamber (Corning, USA) with serum-free medium. The lower compartment of the transwell chamber used serum culture medium. After incubation for 24 h, cells that did not invade in the upper wells were removed gently by cotton swabs. Cells that had passed through the membrane to the lower surface were fixed with 4% paraformaldehyde for 15min and then stained using crystal violet for 10min. Images were obtained using an inverted optical microscope (Nikon ECLIPSE TS100,Japan).These data were quantified using ImageJ software.

Cell proliferation assay

The proliferation of HPV-PZ-7 and PC 3 cells under different substrate stiffness was detected by CCK-8 assay. The cells were incubated on PAA hydrogels of different stiffness for 48h, digested and inserted into 96-well plates at a rate of 1×10^4 cells per well. The cells were incubated for 12h, 24h, 48h and 72h, respectively. The cells were then treated with 10ul CCK-8 reagent (Sigma-Aldrich)/100ul medium for 1 h.

The optical density (OD) values were then evaluated at 450nm using a microplate reader (Bio-Rad).

Cell morphology assay

HPV-PZ-7 and PC 3 cells were inoculated into PAA hydrogel substrates with different stiffness at a density of 1×10^4 cells/ mL for 48h, and the cell morphology of the substrates with different stiffness was obtained by inverted optical microscope (Nikon ECLIPSE TS100, Japan). Illustrator software was used to analyze cell morphology and size.

Atomic force microscope (AFM)

The elastic modulus of cells (2×10^4 cells/mL) that cultured on PAA gel with different stiffness for 48 h was determined by AFM (JPK NanoWizard Ⅲ, Germany) equipped with an inverted optical microscope (Leica, Germany). Measurements were performed in 37°C maintained in a Petri dish heater (JPK instrument, Berlin Germany)for 2h to prevent damage to the cell state. Before the experiment, the thermal noise method was used to adjust the cantilever spring constant, and then the experiment was carried out in contact mode. The AFM probe (MLCT probe , Bruker, USA) slightly contacted the cell surface and maintained a constant force. Indentation area (3 μm × 3 μm) was selected at the nucleus region where 36 force curves were recorded for each cell in force spectroscopy mode. The indentation force of 1 nN, spring constant values of 0.01 $N\cdot m^{-1}$, Z length 5μm and an approach speed of approximately 2 $\mu m\cdot s^{-1}$ were employed in all AFM experiments. Maintain the same parametric parameters for all cells measured. The elastic modulus was acquired based on the Hertz model. Viscosity was calculated using the method proposed by Rebelo's group which combining the traditional method with the AFM retraction force

curve[41, 42].This method can be used to measure young's modulus and calculate cell viscosity directly from the measured force spectrum.

For morphometric analysis, cells (2×10^4 cells/mL) cultured on PAA gel with different stiffness for 48 h were fixed in 4% paraformaldehyde for 15min and washed with 2mL PBS, then subjected to observed in QI working mode with Setpoint 1nN, Z Length 2000nm and Pixel Time 50 ms. Topography scanning at each pixel position (128×128) of the selected area (50 μm×50 μm) to obtain high-resolution surface topography features of cells. The profiles of cells were extracted from topographic images using Image J software. 3D reconstitution of topographic images was performed using JPK software. Maintain the same parametric parameters for all cells measured.

Confocal microscopy

Cells (5×10^4 cells/ mL) were plated onto polyacrylamide gel substrates and fixed in 4% paraformaldehyde for 15 min at room temperature. Then, they were washed with PBS, and permeabilized in 0.1% Triton X-100 for 10 min. The cells were washed with PBS, and incubated with ActinGreen (KeyGEN, BioTECH) for 40 min away from light. The samples were washed with PBS. Fluorescence images were obtained using an inverted optical microscope (Leica, Germany) with 488 laser lines. Images were linearly analysed and pseudo-coloured using ImageJ analysis software.

Statistical analysis

All representative qualitative data were replicated in at least three separate biological replicates. Student’s t-test and one–way ANOVA analyses were performed, as indicated in the captions of the figures and supplementary figures, with GraphPad Prism 6.0. Means are presented ± standard deviation of multiple measurements and statistical significance was considered at $P < 0.05$.

Funding

This work was supported by the National Key Basic Research Program of China (973 project) under grant no. 2015CB352006, the National Natural Science Foundation of China under grant no. 61335011, the Program for Changjiang Scholars and Innovative Research Team in University under grant no. IRT_15R10, the scientific research innovation team construction program of Fujian Normal University under grant no. IRTL1702, Special Funds of the Central Government Guiding Local Science and Technology Development under grant no. 2017L3009, and the Natural Science Foundation of Fujian Province under grant nos. 2018J01814 and 2018J05102, the Fujian Province Educational Project A (JAT170127) and the Health and Family Planning Scientific Research Personnel Training Project of Fujian Province under grant no. 2018-ZQN-45.

References

1. Mbbc, A.; Is, B.; Jae, C.; Fb, B.; Aj, A. *European Urology*.**2020**, *77* (1), 38-52.doi:10.1016/j.eururo.2019.08.005.
2. Swami, U.; McFarland, T. R.; Nussenzveig, R.; Agarwal, N. *Trends Cancer*.**2020**, *6* (8), 702-715.doi:10.1016/j.trecan.2020.04.010.
3. Litwin, M. S.; Tan, H. J. *Jama*.**2017**, *317* (24), 2532-2542.doi:10.1001/jama.2017.7248.
4. Hamdy, F. C.; Donovan, J. L.; Lane, J. A.; Mason, M.; Metcalfe, C.; Holding, P.; Davis, M.; Peters, T. J.; Turner, E. L.; Martin, R. M.; et al. *N Engl J Med*.**2016**, *375* (15), 1415-1424.doi:10.1056/NEJMoa1606220.
5. Teo, M. Y.; Rathkopf, D. E.; Kantoff, P. *Annu Rev Med*.**2019**, *70* (1), 479-499.doi:10.1146/annurev-med-051517-011947.
6. Force, U. S. P. S. T.; Grossman, D. C.; Curry, S. J.; Owens, D. K.; Bibbins-Domingo, K.; Caughey, A. B.; Davidson, K. W.; Doubeni, C. A.; Ebell, M.; Epling, J. W., Jr.; et al. *Jama*.**2018**, *319* (18), 1901-1913.doi:10.1001/jama.2018.3710.
7. Ghosh, D.; Dawson, M. R. *Advances in experimental medicine and biology*.**2018**, *1092*, 69-90.doi:10.1007/978-3-319-95294-9_5.
8. Kalli, M.; Stylianopoulos, T. *Front Oncol*.**2018**, *8*, 55.doi:10.3389/fonc.2018.00055.
9. Gil-Redondo, J. C.; Weber, A.; Zbiral, B.; Vivanco, M. D.; Toca-Herrera, J. L. *J Mech Behav Biomed Mater*.**2022**, *125*, 104979.doi:10.1016/j.jmbbm.2021.104979.

10. Qin, X.; Lv, X.; Li, P.; Yang, R.; Xia, Q.; Chen, Y.; Peng, Y.; Li, L.; Li, S.; Li, T.; et al. *Biochimica et biophysica acta. Molecular basis of disease*.**2020**, *1866* (3), 165625.doi:10.1016/j.bbadis.2019.165625.
11. Peng, Y.; Chen, Z.; Chen, Y.; Li, S.; Jiang, Y.; Yang, H.; Wu, C.; You, F.; Zheng, C.; Zhu, J.; et al. *Acta Biomater*.**2019**, *88*, 86-101.doi:10.1016/j.actbio.2019.02.015.
12. Dai, J.; Qin, L.; Chen, Y.; Wang, H.; Lin, G.; Li, X.; Liao, H.; Fang, H. *J Mech Behav Biomed Mater*.**2019**, *90*, 226-238.doi:10.1016/j.jmbbm.2018.10.012.
13. Rice, A.; Cortes, E.; Lachowski, D.; Cheung, B.; Karim, S.; Morton, J.; Del Rio Hernandez, A. *Oncogenesis*.**2017**, *6* (7), e352-e352.doi:10.1038/oncsis.2017.54.
14. Dong, Y. Y.; Zheng, Q. D.; Wang, Z. M.; Lin, X. H.; You, Y.; Wu, S. F.; Wang, Y. H.; Hu, C.; Xie, X. Y.; Chen, J.; et al. *Journal of Hematology & Oncology*.**2019**, *12* (1), 1-15.doi:10.1186/S13045-019-0795-5.
15. Liu, Z.; Wang, L.; Xu, H.; Du, Q.; Li, L.; Wang, L.; Zhang, E. S.; Chen, G.; Wang, Y. *Adv Sci (Weinh)*.**2020**, *7* (15), 1903583.doi:10.1002/advs.201903583.
16. Dufrene, Y. F.; Ando, T.; Garcia, R.; Alsteens, D.; Martinez-Martin, D.; Engel, A.; Gerber, C.; Muller, D. J. *Nature Nanotechnology*.**2017**, *12* (4), 295-307.doi:10.1038/Nnano.2017.45.
17. Liang, X. T.; Liu, S.; Wang, X. C.; Xia, D.; Li, Q. *Beilstein Journal of Nanotechnology*.**2021**, *12* (1), 1372-1379.doi:10.3762/bjnano.12.101.
18. Krieg, M.; Flaschner, G.; Alsteens, D.; Gaub, B. M.; Roos, W. H.; Wuite, G. J. L.; Gaub, H. E.; Gerber, C.; Dufrene, Y. F.; Muller, D. J. *Nature Reviews Physics*.**2019**, *1* (1), 41-57.doi:10.1038/s42254-018-0001-7.
19. Chen, M. D.; Zeng, J. S.; Ruan, W. W.; Zhang, Z. H.; Wang, Y. H.; Xie, S. S.; Wang, Z. C.; Yang, H. Q. *Beilstein Journal of Nanotechnology*.**2020**, *11* (1), 568-582.doi:10.3762/bjnano.11.45.
20. Tang, X.; Ruan, W.; Zeng, J.; Chen, M.; Wang, Y.; Yang, H. In *Eleventh International Conference on Information Optics and Photonics*, 2019; International Society for Optics and Photonics: Vol. 11209, p 112093S. DOI: 10.1117/12.2548958.
21. Rouvière, O.; Melodelima, C.; Dinh, A. H.; Bratan, F.; Souchon, R. *European Radiology*.**2016**, *27* (5), 1858-1866.doi:10.1007/s00330-016-4534-9.
22. Zhai, L.; Madden, J.; Foo, W. C.; Mouraviev, V.; Polascik, T. J.; Palmeri, M. L.; Nightingale, K. R. *Ultrasonic Imaging*.**2010**, *32* (4), 201.doi:10.1177/016173461003200401.
23. Junker, D.; De Zordo, T.; Quentin, M.; Ladurner, M.; Bektic, J.; Horniger, W.; Jaschke, W.; Aigner, F. *Biomed Research International*.**2014**, *2014*, 180804.doi:10.1155/2014/180804.
24. Prauzner-Bechcicki, S.; Raczkowska, J.; Madej, E.; Pabijan, J.; Lukes, J.; Sepitka, J.; Rysz, J.; Awsiuk, K.; Bernasik, A.; Budkowski, A.; et al. *J Mech Behav Biomed Mater*.**2015**, *41*, 13-22.doi:10.1016/j.jmbbm.2014.09.020.
25. Grasset, E. M.; Bertero, T.; Bozec, A.; Friard, J.; Bourget, I.; Pisano, S.; Lecacheur, M.; Maiel, M.; Bailleux, C.; Emelyanov, A.; et al. *Cancer Res*.**2018**, *78* (18), 5229-5242.doi:10.1158/0008-5472.CAN-18-0601.
26. Tang, R. Z.; Gu, S. S.; Chen, X. T.; He, L. J.; Wang, K. P.; Liu, X. Q. *ACS Appl Mater Interfaces*.**2019**, *11* (16), 14660-14671.doi:10.1021/acsami.9b03572.
27. Kyung; Sook; Kim; Chang; Hoon; Cho; Eun; Kuk; Park; Min-Hyung. *PLoS ONE*.**2012**, *7* (1), e30066.doi:10.1371/journal.pone.0030066.
28. Ng, M. R.; Besser, A.; Danuser, G.; Brugge, J. S. *Journal of Cell Biology*.**2012**, *199* (3), 545-563.doi:10.1083/jcb.201207148.
29. Mattila, P. K.; Lappalainen, P. *Nature reviews. Molecular cell biology*.**2008**, *9* (6), 446-454.doi:10.1038/nrm2406.

30. Garcin, C.; Straube, A. *Essays in Biochemistry*.**2019**, *63* (5), 509-520.doi:10.1042/ebc20190016.
31. Carlier, M. F.; Pantaloni, D. *The Journal of biological chemistry*.**2007**, *282* (32), 23005-23009.doi:10.1074/jbc.R700020200.
32. Pollard, T. D.; Borisy, G. G. *Cell*.**2003**, *112* (4), 453-465.doi:10.1016/s0092-8674(03)00120-x.
33. Coughlin, M. F.; Stamenovic, D. *J Biomech Eng*.**1998**, *120* (6), 770-777.doi:10.1115/1.2834892.
34. Rianna, C.; Radmacher, M. *Nanoscale*.**2017**, *9* (31), 11222-11230.doi:10.1039/c7nr02940c.
35. Fischer, T.; Wilharm, N.; Hayn, A.; Mierke, C. T. *Convergent Science Physical Oncology*.**2017**, *3* (4), 044003.doi:10.1088/2057-1739/aa8bbb.
36. Lekka, M.; Laidler, P.; Gil, D.; Lekki, J.; Stachura, Z.; Hrynkiewicz, A. Z. *European biophysics journal : EBJ*.**1999**, *28* (4), 312-316.doi:10.1007/s002490050213.
37. Li, Q. S.; Lee, G. Y.; Ong, C. N.; Lim, C. T. *Biochemical and biophysical research communications*.**2008**, *374* (4), 609-613.doi:10.1016/j.bbrc.2008.07.078.
38. Ketene, A. N.; Schmelz, E. M.; Roberts, P. C.; Agah, M. *Nanomedicine : nanotechnology, biology, and medicine*.**2012**, *8* (1), 93-102.doi:10.1016/j.nano.2011.05.012.
39. Kim, D. H.; Xing, T. S.; Yang, Z. B.; Dudek, R.; Lu, Q.; Chen, Y. H. *Journal of Clinical Medicine*.**2018**, *7* (1), 1.doi:10.3390/Jcm7010001.
40. Tse, J. R.; Engler, A. J. *Curr Protoc Cell Biol*.**2010**, *Chapter 10* (1), Unit 10 16.doi:10.1002/0471143030.cb1016s47.
41. Rebelo, L. M.; de Sousa, J. S.; Mendes Filho, J.; Radmacher, M. *Nanotechnology*.**2013**, *24* (5), 055102.doi:10.1088/0957-4484/24/5/055102.
42. Wang, Y.; Xu, C.; Jiang, N.; Zheng, L.; Zeng, J.; Qiu, C.; Yang, H.; Xie, S. *Scanning*.**2016**, *38* (6), 558-563.doi:10.1002/sca.21300.